



Effects of He radiation on cavity distribution and hardness of bulk nanolayered Cu-Nb composites



L.X. Yang^a, S.J. Zheng^{a,*}, Y.T. Zhou^a, J. Zhang^b, Y.Q. Wang^c, C.B. Jiang^a, N.A. Mara^c, I.J. Beyerlein^d, X.L. Ma^a

^a Shenyang National Laboratory for Materials Science, Institute of Metal Research, Chinese Academy of Sciences, Shenyang 110016, China

^b School of Energy Research, Xiamen University, Xiamen 361005, China

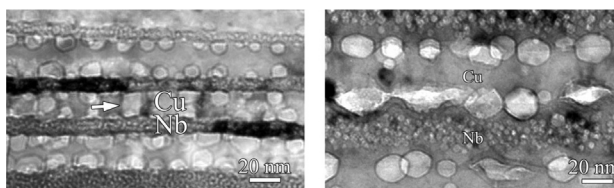
^c LANL Institute for Materials Science and the Center for Integrated Nanotechnologies, Los Alamos National Laboratory, Los Alamos, NM 87545, USA

^d Mechanical Engineering Department, Materials Department, University of California at Santa Barbara, Santa Barbara, CA 93106, USA

HIGHLIGHTS

- Effects of He radiation temperature, fluence, and layer thickness on damage of ARB nanolayered Cu-Nb composites have been investigated.
- Whether cavities cross the interface depends on layer thickness and temperature.
- He radiation could generate softening mainly owing to recovery of dislocations.

GRAPHICAL ABSTRACT



ARTICLE INFO

Article history:

Received 2 November 2016

Received in revised form

13 February 2017

Accepted 14 February 2017

Available online 21 February 2017

Keywords:

Interface

Cavity

Softening

Radiation

Nanolayered composite

ABSTRACT

Interface engineering is an important strategy for developing radiation tolerant materials. In prior work, bulk nanolayered composites fabricated by accumulative roll bonding (ARB) showed outstanding radiation resistance. However, the effects of layer thickness and radiation conditions on damage distributions and their effect on hardness have not been explored. Here, we use transmission electron microscopy (TEM) and nanoindentation to investigate the effects of radiation on the distribution of radiation-induced cavities and post-radiation hardness in ARB nanolayered Cu-Nb composites. We show that whether the cavities cross the interface depends on layer thickness and temperature, and that, remarkably, radiation could generate softening, not always hardening. We posit that the softening mainly results from the recovery of dislocations stored in the crystal after the bulk forming ARB processing due to He radiation and this phenomenon offsets radiation-induced hardening as layers become finer and temperatures rise.

© 2017 Elsevier B.V. All rights reserved.

1. Introduction

Structural materials in nuclear reactors suffer damage due to long-term exposure to high temperatures, high stress, corrosion, and radiation. Voids and bubbles, which are some of the major forms of irradiation-induced damage, are generated by the He

radiation that accompanies endothermic (n, α) reactions. These He bubbles and voids lead to detrimental changes in the material microstructure, dimensions, and structural performance, such as swelling, hardening, and embrittlement [1–6]. Hardening, for example, can be severe. In 316LN stainless steel, He radiation that leaves peak He concentrations of 10% in the material has been reported to cause enhancements in hardening ΔH up to 90% percent [7].

The enhancement in hardness, ΔH , is thought to result from the

* Corresponding author.

E-mail address: sjzheng@imr.ac.cn (S.J. Zheng).

bubbles or voids, or hereinafter generically called cavities, remaining after irradiation and their ability to hinder dislocation motion. Accordingly, ΔH would increase with the size and/or density of cavities in the crystal as they would present larger and/or more frequent obstacles to dislocation glide. This relationship between cavity properties and ΔH has been described by the Friedel-Kroupa-Hirsch (FKH) relation [8,9],

$$\Delta H \approx 3\Delta\sigma_{cavity} = \frac{1}{8}MGbdN_{cavity}^2 \quad (1)$$

where M is Taylor factor reflecting crystal orientation; G is the shear modulus (GPa); b is the Burgers vector (nm) of the dislocation; d is the cavity diameter (nm) and N is the cavity density (m^{-3}). Thus, for a given material, the larger the cavity size and/or cavity density in the crystal, the higher ΔH is.

Extensive studies have demonstrated that interfaces and grain boundaries can serve as excellent sinks for point defects [10,11], and can store He ions efficiently [12], therefore reducing cavity sizes and densities in the adjoining crystals and minimizing post-irradiation swelling and hardening [13–16]. Using deposited Cu-Nb multilayer thin films as an interface-dominant model material system, Li et al. [16] demonstrated that when the layer thickness (or interface spacing) reduced from 70 nm to 5 nm, the He cavity volume fraction within the layers decreased with concomitant reductions in hardening enhancement ΔH . This study is just one of the many examples suggesting that introduction of biphasic interfaces can be an important strategy to design radiation-resistant materials.

Most of these studies on the promising mitigation effects of biphasic interfaces were carried out in thin films fabricated by bottom-up techniques, such as physical vapor deposition [15]. Recently, simultaneous high strength and outstanding thermal stability were demonstrated in bulk nanolayered Cu-Nb composites fabricated by a top-down processing method, called accumulative roll bonding (ARB Cu-Nb) [15,17,18]. Unlike bottom-up deposition techniques, the ARB process can be scaled up to manufacture sheet metal in quantities suitable for structural components. Microscopic analyses revealed that just like the prior Cu-Nb nanocomposite studies, no voids formed in the interfaces and only within the crystalline layers, suggesting that void formation was hindered in the interfaces [19]. Moreover, the voids that formed in the crystal near the interfaces tended to stay on the Cu side of the interface and predominately where non-parallel misfit dislocations in the interface intersected [20]. The preference of the Cu phase arises because Cu has a smaller surface energy than Nb and wets the regions of highest interface energy, which is where the misfit dislocations in the Cu-Nb interface intersect [20,21]. Thus, like the thin films, the bulk sheet material exhibits similar behavior, but with it, we have much more versatility in processing and potential for achieving target interface properties [18]. Furthermore, the correlation between void spacing along the boundaries and interface dislocation structure suggests that the distribution of He bubbles or voids could be tuned by engineering the interface.

It should be mentioned that in these previous studies, He was directly implanted into transmission electron microscope (TEM) samples [19,20]. TEM samples are thin films, in which the thicknesses of observable regions are usually less than 100 nm. For such fine thicknesses, He ions transmit across the samples and generating damage in their wake. The type of damage, however, should be different from that generated when the He ions terminate within the bulk material.

Also, as mentioned, temperature, fluence, and grain size (layer thickness) are dominant factors influencing cavity size and distribution [1,4,5,22], and hence ΔH . Such effects have not been

investigated in these bulk structural Cu-Nb composites. Here, in order to evaluate the radiation resistance of bulk Cu-Nb composites, we investigate interface effects on cavity distribution and ΔH . As the damage could include either bubbles or voids, hereinafter we use the term cavity to generically encompass both types of damage. Our analyses find that whether the cavities cross the interface depends on layer thickness and temperature, and that, remarkably, radiation could generate softening, not hardening. We rationalize that softening results from annihilation of the dislocations stored within the crystal after the bulk forming ARB processing by interactions with radiation-induced defects, as well as from thermal annealing. For finer layers, such as < 20 nm, there is less room for dislocations to move and dislocation annihilation at cavities dominates over dislocation blockage by cavities. These effects, such as cavity formation in interfaces and softening, were not reported before for nanolayered composites, since other temperatures and fluence conditions were not considered.

2. Materials and methods

The ARB Cu-Nb composites used for this work started with polycrystalline sheets of reactor grade Nb (99.97% pure, ATI-Wah Chang) and oxide-free high conductivity Cu (99.99% pure, Southern Copper and Supply) in a 50-50% volume ratio. Details on the ARB process, which included repeatedly cleaning, stacking, roll-bonding, and cutting, can be found in Ref. [17]. ARB Cu-Nb composites chosen for this radiation study are 300 μm thick sheets with nominal layer thicknesses of 16 and 58 nm respectively. These materials have similar grain structures, with one grain spanning the layer thickness, and textures [23]. He-ion irradiation was conducted using a Danfysik 200 kV ion implanter at Los Alamos National Laboratory at room temperature (RT) and 450 °C. All the samples were mounted on a stage with cooling and heating systems which can monitor the temperature precisely. To reach a fluence of 2×10^{17} ions/cm², the radiation process lasted for about 5 h. The SRIM calculation for the radiation of the 58 nm sample shown in Fig. 1a indicates that the most intense damage and He concentration are about 16 dpa and 11 at.% at depths of about 500 and 550 nm respectively. The SRIM calculations for the 16 nm samples showed a similar damage and He-concentration profile vs. depth as those of the 58 nm samples and hence are not shown here for compactness. For comparison, radiation with fluences of 2×10^{17} ions/cm² and 6.5×10^{17} ions/cm² at RT were performed on the 58 nm ARB Cu-Nb composites, which required about 10 h. More detailed information for the sample can be found in Table 1.

To investigate the distribution of voids and bubbles after irradiation, TEM samples were prepared by a conventional cross-sectioning method, consisting of low-speed saw cutting, mechanical polishing, dimpling, and ion milling on a Gatan precision ion polishing system (PIPS) operated at 3.5 kV. TEM was performed on a Tecnai F30 (FEI) operated at 300 kV.

To test for hardening enhancements, the hardness before and after radiation was measured using nano-indentation on a Nano-indenter G200 (Agilent). Indents were performed to a depth of 500 nm with a target strain rate of 0.05 s⁻¹. Hardness measurements were made in the continuous stiffness measurement mode. Average hardness values were calculated from 16 separate indents with a depth range of 460–480 nm.

Under the He radiation conditions applied here, He concentrations can be detected up to depths of 400–700 nm in both the 16 and 58 nm ARB Cu-Nb samples. Taking the 58-RT sample as an example, as shown in Fig. 1b, the maximum He concentration appears at a depth of 550 nm, which is consistent with the SRIM calculations. This He distribution also agrees well with a previous study using the same He radiation conditions [24]. Hereinafter, we

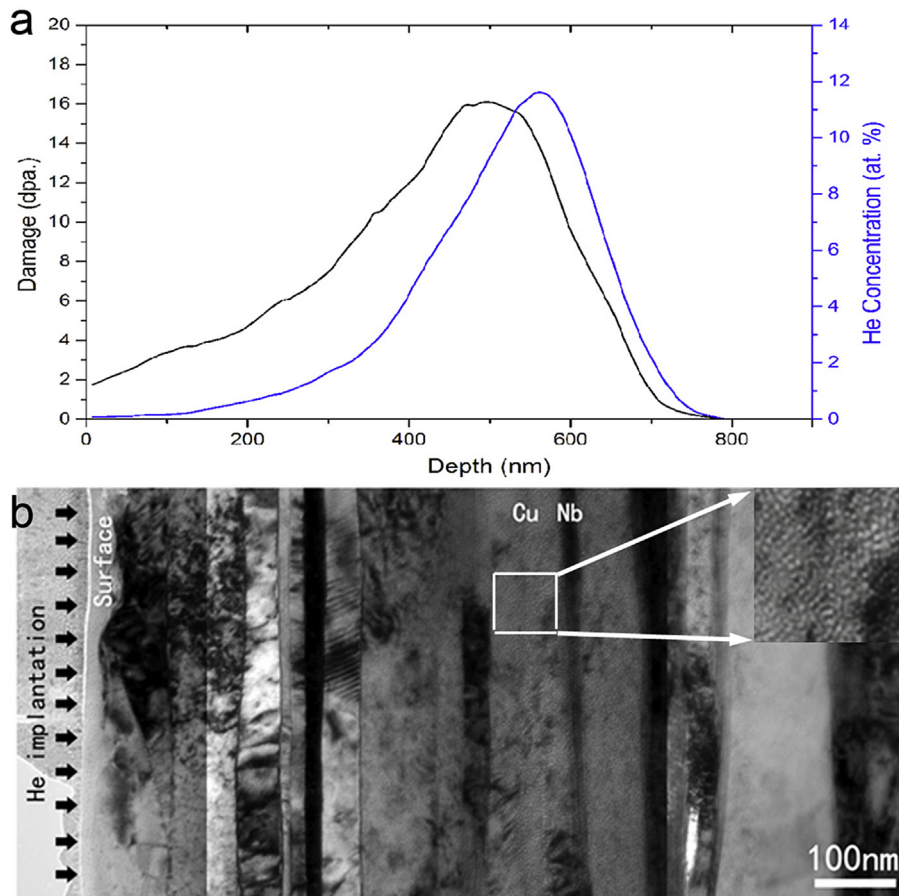


Fig. 1. (a) SRIM calculation of damage and He concentration via depth, (b) cross-section TEM image of the 58-RT sample, in which the local enlarged region marked with a white square shows the concentrated He bubbles. The SRIM calculations and TEM results of damage and He concentration via depth for the other samples are similar.

Table 1
Sample information.

Sample name	Layer thickness (nm)	Radiation fluence (ions/cm ²)	Radiation temperature
16 nm-AR (as rolled)	16	none	none
16 nm-RT	16	2×10^{17}	Room temperature (RT)
16 nm-450 °C	16	2×10^{17}	450 °C
58 nm-AR (as rolled)	58	none	none
58 nm-RT	58	2×10^{17}	Room temperature (RT)
58 nm-RT-6.5	58	6.5×10^{17}	Room temperature (RT)
58 nm-450 °C	58	2×10^{17}	450 °C

focus on the structural evolution at depths where He ions have presumably concentrated.

3. Results

Fig. 2 shows TEM images of the cavity distribution in the 16 nm ARB Cu-Nb sample radiated at both RT and 450 °C. In this fine-layered composite, He cavities are found within the layers and along the Cu-Nb interface but not across or within them. We refer to this cavity configuration as a *confined-layered distribution*. After RT irradiation (Fig. 2a), He cavities appear as the bright spots approximately 1 nm in diameter in both the Nb and Cu layers. The cavity density is larger and the cavities are bigger along the Cu-Nb interfaces than within the layer interior, suggesting that the interfaces can act as effective traps for He ions. Moreover, these interface-touching cavities are found in the Cu layers than in the Nb layers, which is consistent with prior observations on another

material system, Cu-Ag, as well as the more general theoretical prediction based on interface wetting of He cavities [12,20].

Fig. 2b shows that the same confined-layered distribution develops in the 16 nm ARB Cu-Nb sample radiated at the higher temperature 450 °C. After radiation at 450 °C, the cavities in the Nb and Cu are larger than at RT, being about 1–2 nm in Nb and significantly larger, approximately 10 nm in the Cu. Again, as in the RT sample, the cavities do not form within the layers. Some cavities even span the Cu layer as indicated by an arrow in Fig. 2b or wet the interfaces, as shown in the bottom Cu layer in Fig. 2b, but nonetheless, remain confined within the Cu layers. This observation is consistent with a previous study of the confinement effect of the interface on He cavities in Cu-Nb multilayers fabricated via physical vapor deposition (PVD) with layer thickness of 5 and 120 nm [25].

In the foregoing cases, the interface spacing was very fine and the cavities did not form in the interfaces. First, to investigate the effects of interface spacing on cavity density, we repeated the study

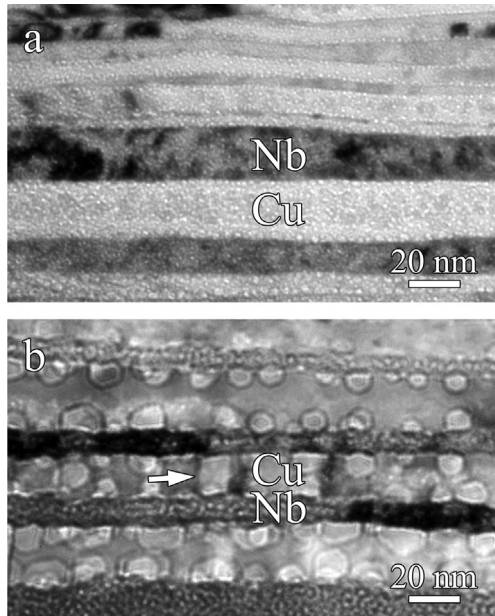


Fig. 2. Microstructures of 16 nm ARB Cu-Nb composites after He radiation: (a) 16-RT, (b) 16–450.

with 58 nm ARB Cu-Nb composites after He radiation at both RT and 450 °C. Fig. 3a shows the TEM image displaying the typical distribution of cavities seen in the 58 nm-RT sample. As shown in Fig. 3a, the cavities exhibit a similar confined-layered distribution as the RT 16 nm samples. The average cavity size is about 1 nm and the cavities are found in both the Cu and Nb layers. The cavities in the 16 nm composites bear the same properties, indicating that the layer thickness, i.e. interface density, apparently does not affect the distribution of cavities and their size at RT.

Second, to explore the dependence of this interface effect on fluence, we studied the distribution of cavities in the 58 nm-RT samples that were irradiated at a higher fluence of 6.5×10^{17} ions/cm². From the image shown in Fig. 3b, it is clear that, as the fluence increases from 2×10^{17} to 6.5×10^{17} ions/cm², the cavity size along the Cu-Nb interfaces increases to about 6 nm, a trend that generally is not surprising. Thus, based on the FKH relation, we can expect that these crystalline cavities would lead to an increase in hardening compared to the unirradiated sample. Yet, we note that the cavities in both the Cu and Nb layers still have a confined-layered distribution. Thus, even increasing the fluence does not cause cavities to form within the interfaces but causes them to only grow bigger at RT.

Last, we examine the effects of temperature on the distribution of cavities. It is found that unlike the 16 nm ARB material, in the 58 nm ARB Cu-Nb composites radiated at high temperature, the cavities cross or form within the Cu-Nb interfaces. This defect configuration, in which cavities cross the interface, will be referred to as a *cross-layered distribution*. As shown in Fig. 3c of the 58–450 sample, the cavity size, which is about 3 nm in the Nb layers, is much bigger than that in the 58 nm-RT and the 58 nm-RT-6.5 samples. Most interestingly, the cavities cross the Cu-Nb interfaces, and possess a much larger average size of 16 nm, while there are almost no cavities in the Cu layers. This result suggests that a *cross-layered distribution* can form provided that the temperatures are high and layers are thick enough.

In all irradiated samples, cavities formed in either or both the Cu and Nb layers. It can, therefore, be expected that radiation hardening would occur. As mentioned, enhancements in hardening after He irradiation are common in metals and have been reported in

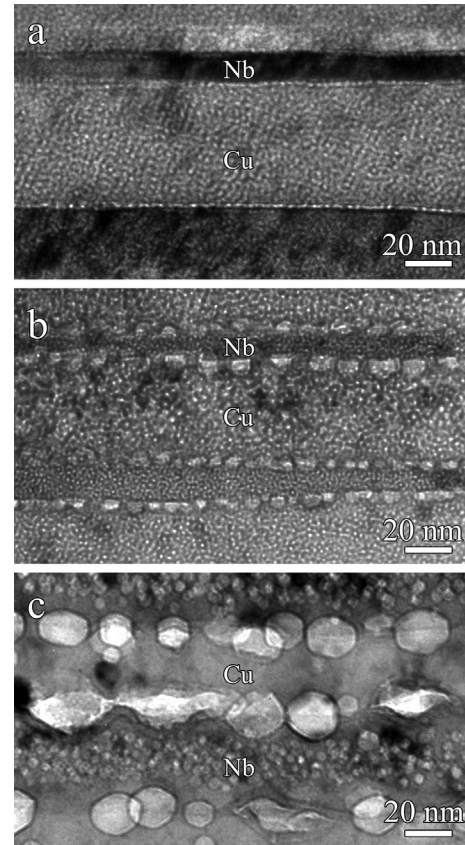


Fig. 3. Microstructures of 58 nm ARB Cu-Nb composites after He radiation: (a) 58-RT, (b) 58-RT-6.5, (c) 58–450.

PVD Cu-Nb nanolaminates in prior work [6,7]. Next, we examine the hardness of these 16 nm and 58 nm nanolaminates before and after irradiation. Fig. 4 shows the results of hardness tests on the He-irradiated 16 nm and 58 nm ARB Cu-Nb composites. Beginning with the finer-layered 16 nm composite, we observe that remarkably these samples exhibit softening rather than hardening after He-irradiation at both RT and 450 °C. The unirradiated 16-nm sample has the highest hardness of 4.95 ± 0.29 GPa among all samples. After RT and 450 °C He irradiation, it softened to $4.73 \pm$

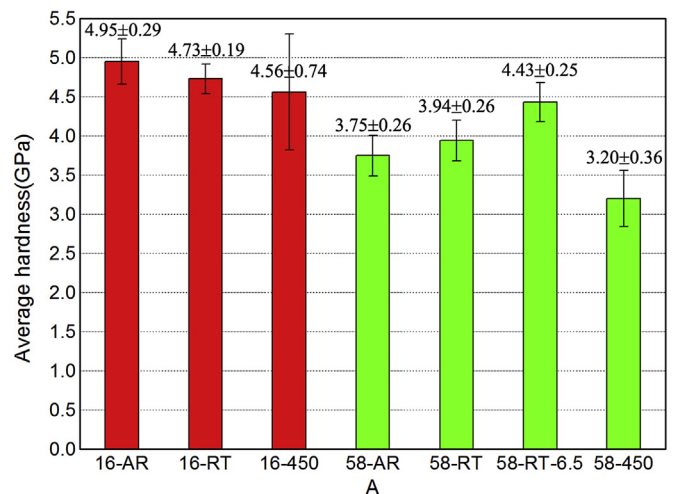


Fig. 4. Hardness evolution of the 16 nm and 58 nm ARB Cu-Nb composites.

0.19 GPa and 4.56 ± 0.74 GPa, respectively. Like the other fine-layered Cu-Nb composites made by PVD, these composites formed cavities in the layers and not interfaces, as seen in Fig. 2. The cavity size even increased with an increase in radiation temperature from RT to 450 °C, but yet the material also softened at the higher temperature.

In the 58 nm samples, we find that the commonly observed hardening takes place after room temperature He radiation. The hardness of the unirradiated 58 nm sample, which is 3.75 ± 0.26 GPa, increases to 3.94 ± 0.26 GPa and 4.43 ± 0.25 GPa in the 58-RT and 58-RT-6.5 samples, respectively. The enhancement ΔH is higher for the sample exposed to the higher fluence, which would be anticipated since the higher fluences were found to lead to larger cavities (Fig. 3). Thus, unlike the 16 nm samples, the 58 nm samples, which also exhibited a confined-layered cavity distribution, followed conventional expectation. Moreover, the interfaces and textures in the 58 nm and 16 nm are very similar [17]. Therefore the unusual softening seen in the 16 nm sample could be a layer thickness effect.

Finally, we note the interesting observation that the irradiated 58 nm–450 °C sample also shows softening relative to the 58 nm-AR sample. Thus it responds to radiation in a similar manner as the 16 nm-RT and 16 nm–450 °C samples. In this case, however, the cavity distribution was distinct from the others, lying within the interfaces and Nb layer but not the Cu layer. To summarize, we see an unusual post-irradiation softening in the 16 nm samples radiated at RT and 450 °C, which had a confined-layer distribution and the 58 nm sample radiated at 450 °C, which had a cross-layer distribution.

4. Discussion

The well-known phenomenon of He cavity induced hardening took place in the 58 nm-RT and 58 nm-RT-6.5 samples. According to the FKH relationship, ΔH would increase linearly with $dN_{cavity}^{2/3}$. Although the increment of cavity density is difficult to determine, the cavities size increases, as shown in Fig. 3a and b, as the fluence increases. As the fluence increases from 2×10^{17} to 6.5×10^{17} ions/cm², the increment of hardness also increases from 5.0% to 18%. Thus, both the fluence and increment of hardness increase about three times, and the linear FKH relation between the fluence and increment of hardness evidently applies in this case.

Post-irradiation softening is an interesting finding in the present work and is not captured by the FKH relation. It presumes that cavities lead to hardening and for the same material composition and texture, only reductions in d and/or N can lead to reductions in hardening. For all layer thickness, nano-sized cavities form as a result of the irradiation, but in most of the cases we tested, softening, not hardening, was found. Specifically softening occurs in both the 16 nm and 58 nm samples irradiated at 450 °C and thus it can happen whether the nano-cavities lie along the interfaces, as in the 16 nm (confined-layer distribution), or across the interfaces, as in the 58 nm–450 °C (cross-layer distribution).

One reason for the softening should be thermal annealing. High temperatures could diminish radiation hardening. It has been reported that the density of bubbles decreases rapidly with increasing temperature [5]. For example, the bubble density was observed to decrease about two orders of magnitude as the temperature increases from RT to a temperature near $0.5 T_m$ [5]. In the present work, 450 °C is close to $0.5 T_m$ of Cu, so it is reasonable that cavity density in the Cu phase of these samples would decrease about two orders of magnitude as well. Also, when the temperature increases from RT to 450 °C, cavity size only increases about one to one and half orders of magnitude as indicated in Figs. 2–3. Although Nb has a T_m of 2477 °C and thus the temperature of 450

°C does not show as strong an effect on hardness as that for Cu, Nb should still display the same trend of hardness change with Cu. So according to the FKH relation, the radiation hardening could be reduced for samples radiated at 450 °C.

Other unusual effects of nano-sized radiation-induced cavities have been reported. Recently, it has been found that nanosized He cavities could improve ductility of a metallic glass with no sacrifice in yield and ultimate tensile strength [26]. Also, Ding et al. [27] has shown a similar ductility enhancement by nanosized He cavities in single crystal Cu, and they rationalized this phenomenon results from He cavities acting as both dislocation sources and shearable obstacles, which promote dislocation storage and reduce dislocation mean free path. However, no softening after irradiation has been reported by far.

The cavities introduce a second type of interface, at which dislocations can be annihilated or nucleated or their glide motion hindered when the material is deformed. In coarser materials, dislocations have other sources and sinks like biphasic interfaces, surfaces, grain boundaries and stored dislocations (substructure, tangles). Usually, nano-sized cavities predominately act as obstacles to dislocation glide, rather than as sources or sinks, enhancing the hardness, as is reflected in the FKH relation. In nanomaterials, however, we speculate that in the cases of post-radiation softening, cavities could play a role as a newly introduced sink for dislocations. Both the ARB Cu-Nb 16 nm and 58 nm nanolayered composites used in the present study were rolled at room temperature without any annealing process, and consequently contained a high density of dislocations as shown in Fig. 5. After He radiation, as shown in Figs. 2 and 3, we find that the dislocation density has decreased dramatically. Similar observations of annihilation of dislocations as a result of interactions between dislocations and point defects induced by radiation have been reported in pure Cu [28] and a Ni-based alloy [29]. Thus, the reduction in hardness could reflect the drop in stored dislocation density. By virtue of the fabrication method, the Cu-Nb samples made by PVD had little to

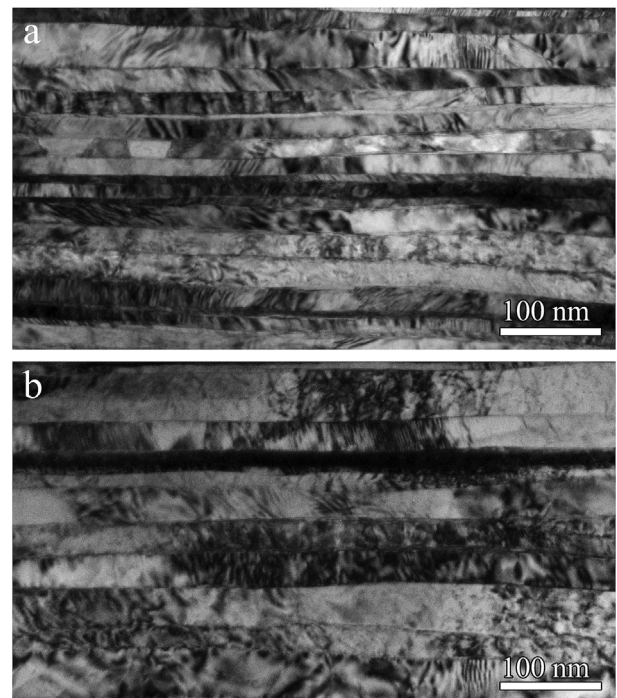


Fig. 5. Microstructures of the ARB Cu-Nb composites before He radiation showing dense dislocations: (a) 16-AR, (b) 58-AR.

no stored dislocation density in the layers. Thus, softening was not seen there. Moreover, when cavity size is big enough to be comparable to the layer thickness, as the cases in both the 16 nm and 58 nm samples irradiated at 450 °C, the cavities may enhance dislocation behavior during plastic deformation. First, although small cavity could harden metallic materials, large cavities are rather weak barriers to dislocations, and even are sources of dislocations owing to their large surface. Second, the high hardness of Cu/Nb composites arises from their semi-coherent interfaces. The disruption of layer interfaces by significantly large cavities could reduce the interface barrier strength to the transmission of dislocations.

We find here that whether or not the softening effect of irradiation dominates apparently depends on layer thickness and temperature. In the 16 nm, dislocation motion is confined by the interface but not the small cavities, and cavities play a role in annihilation of dislocation during radiation, moreover large cavities may contribute to dislocation dominated plastic deformation. Consequently for these finer layers, softening manifests. In the thicker layers of 58 nm, however, dislocation motion is less confined [30] and the obstacle, annihilation, and source effects of cavities compete. At room temperature, the obstacle effect dominates and the conventional post-radiation hardening occurs, but, at higher temperatures, the annihilation and source effects could dominate and the unusual post-radiation softening ensues.

5. Conclusions

In summary, using TEM and nanoindentation, we studied the effects of radiation on the damage state and hardness of bulk Cu-Nb nanolayered composites fabricated by accumulative roll bonding (ARB). The results show that the cavity distribution after radiation, that is whether they form in the layers and/or within the interfaces, is found to depend on nanolayer thickness and radiation temperature. A significant result of this work is the observation of radiation induced softening, in which the hardness decreases rather than the anticipated increases as seen frequently in other metals. The unusual softening is rationalized primarily to annihilation of dislocations stored in the crystal after the bulk forming ARB processing owing to the radiation-induced cavities and thermal annealing. Finer layers and higher temperatures promote recovery of these dislocations over blockage of dislocation motion at the cavities.

Acknowledgements

S. Z. gratefully acknowledges support for this research by “Hundred Talents Project” of Chinese Academy of Sciences, “Thousand Youth Talents Plan” of China, National Natural Science Foundation of China (grant number 51401208), and Shenyang National Laboratory for Materials Science (grant number 2015RP18). This work was performed, in part, at the Center for Integrated Nanotechnologies, an Office of Science User Facility operated for the U.S. Department of Energy (DOE) Office of Science. Los Alamos National Laboratory, an affirmative action equal opportunity employer, is operated by Los Alamos National Security, LLC, for the National Nuclear Security Administration of the U.S. Department of Energy under contract DE-AC52-06NA25396.

References

- [1] K. Farrell, Experimental effects of helium on cavity formation during irradiation – a review, *Radiat. Eff. Defects Solids* 53 (1980) 175–194.

- [2] S.J. Zinkle, W.G. Wolfer, G.L. Kulcinski, L.E. Seitzman, Stability of vacancy clusters in metals. 2. Effect of oxygen and helium on void formation in metals, *Philos. Mag. a-Physics Condens. Matter Struct. Defects Mech. Prop.* 55 (1987) 127–140.
- [3] G.E. Lucas, The evolution of mechanical property change in irradiated austenitic stainless-steels, *J. Nucl. Mater.* 206 (1993) 287–305.
- [4] H. Trinkaus, B.N. Singh, Helium accumulation in metals during irradiation – where do we stand? *J. Nucl. Mater.* 323 (2003) 229–242.
- [5] S.J. Zinkle, 1.03-Radiation-Induced effects on microstructure, in: R.J.M. Konings (Ed.), *Comprehensive Nuclear Materials*, Elsevier, Oxford, 2012, pp. 65–98.
- [6] M.J. Makin, F.J. Minter, Irradiation hardening in copper and nickel, *Acta Metall.* 8 (1960) 691–699.
- [7] J.D. Hunn, E.H. Lee, T.S. Byun, L.K. Mansur, Helium and hydrogen induced hardening in 316LN stainless steel, *J. Nucl. Mater.* 282 (2000) 131–136.
- [8] J. Friedel, CXXX. On the linear work hardening rate of face-centred cubic single crystals, the London, Edinb. Dublin Philos. Mag. J. Sci. 46 (1955) 1169–1186.
- [9] F. Kroupa, P.B. Hirsch, Elastic interaction between prismatic dislocation loops and straight dislocations, *Discuss. Faraday Soc.* 38 (1964) 49–55.
- [10] M.J. Demkowicz, R.G. Hoagland, J.P. Hirth, Interface structure and radiation damage resistance in Cu-Nb multilayer nanocomposites, *Phys. Rev. Lett.* 100 (2008) 136102.
- [11] X.Y. Liu, B.P. Uberuaga, M.J. Demkowicz, T.C. Germann, A. Misra, M. Nastasi, Mechanism for recombination of radiation-induced point defects at inter-phase boundaries, *Phys. Rev. B* 85 (2012).
- [12] A. Kashinath, A. Misra, M.J. Demkowicz, Stable storage of helium in nanoscale platelets at semicoherent interfaces, *Phys. Rev. Lett.* 110 (2013) 086101.
- [13] A. Misra, M.J. Demkowicz, X. Zhang, R.G. Hoagland, The radiation damage tolerance of ultra-high strength nanolayered composites, *Jom* 59 (2007) 62–65.
- [14] X. Zhang, E.G. Fu, A. Misra, M.J. Demkowicz, Interface-enabled defect reduction in He ion irradiated metallic multilayers, *Jom* 62 (2010) 75–78.
- [15] I.J. Beyerlein, A. Caro, M.J. Demkowicz, N.A. Mara, A. Misra, B.P. Uberuaga, Radiation damage tolerant nanomaterials, *Mater. Today* 16 (2013) 443–449.
- [16] N. Li, M. Nastasi, A. Misra, Defect structures and hardening mechanisms in high dose helium ion implanted Cu and Cu/Nb multilayer thin films, *Int. J. Plast.* 32–33 (2012) 1–16.
- [17] S. Zheng, I.J. Beyerlein, J.S. Carpenter, K. Kang, J. Wang, W. Han, N.A. Mara, High-strength and thermally stable bulk nanolayered composites due to twin-induced interfaces, *Nat. Commun.* 4 (2013).
- [18] S.J. Zheng, J.S. Carpenter, R.J. McCabe, I.J. Beyerlein, N.A. Mara, Engineering interface structures and thermal stabilities via SPD processing in bulk nanostructured metals, *Sci. Rep.* 4 (2014) 4226.
- [19] W.Z. Han, M.J. Demkowicz, N.A. Mara, E.G. Fu, S. Sinha, A.D. Rollett, Y.Q. Wang, J.S. Carpenter, I.J. Beyerlein, A. Misra, Design of radiation tolerant materials via interface engineering, *Adv. Mater.* 25 (2013) 6975–6979.
- [20] S. Zheng, S. Shao, J. Zhang, Y. Wang, M.J. Demkowicz, I.J. Beyerlein, N.A. Mara, Adhesion of voids to bimetal interfaces with non-uniform energies, *Sci. Rep.* 5 (2015) 15428.
- [21] S.J. Zheng, I.J. Beyerlein, J. Wang, J.S. Carpenter, W.Z. Han, N.A. Mara, Deformation twinning mechanisms from bimetal interfaces as revealed by in situ straining in the TEM, *Acta Mater.* 60 (2012) 5858–5866.
- [22] G.M. Cheng, W.Z. Xu, Y.Q. Wang, A. Misra, Y.T. Zhu, Grain size effect on radiation tolerance of nanocrystalline Mo, *Scr. Mater.* 123 (2016) 90–94.
- [23] I.J. Beyerlein, J.R. Mayeur, R.J. McCabe, S.J. Zheng, J.S. Carpenter, N.A. Mara, Influence of slip and twinning on the crystallographic stability of bimetal interfaces in nanocomposites under deformation, *Acta Mater.* 72 (2014) 137–147.
- [24] W.Z. Han, N.A. Mara, Y.Q. Wang, A. Misra, M.J. Demkowicz, He implantation of bulk Cu-Nb nanocomposites fabricated by accumulated roll bonding, *J. Nucl. Mater.* 452 (2014) 57–60.
- [25] K. Hattar, M.J. Demkowicz, A. Misra, I.M. Robertson, R.G. Hoagland, Arrest of He bubble growth in Cu-Nb multilayer nanocomposites, *Scr. Mater.* 58 (2008) 541–544.
- [26] R. Lontas, X.W. Gu, E.G. Fu, Y.Q. Wang, N. Li, N. Mara, J.R. Greer, Effects of helium implantation on the tensile properties and microstructure of Ni73P27 metallic glass nanostructures, *Nano Lett.* 14 (2014) 5176–5183.
- [27] M.-S. Ding, J.-P. Du, L. Wan, S. Ogata, L. Tian, E. Ma, W.-Z. Han, J. Li, Z.-W. Shan, Radiation-induced helium nanobubbles enhance ductility in submicron-sized single-crystalline copper, *Nano Lett.* 16 (2016) 4118–4124.
- [28] C.J. Meechan, Annealing of cold-worked copper by electron irradiation, *J. Appl. Phys.* 28 (1957) 197–200.
- [29] H.C. Chen, D.H. Li, R.D. Lui, H.F. Huang, J.J. Li, G.H. Lei, Q. Huang, L.M. Bao, L. Yan, X.T. Zhou, Z.Y. Zhu, Ion irradiation induced disappearance of dislocations in a nickel-based alloy, *Nucl. Instrum. Methods Phys. Res. Sect. B-Beam Interact. Mater. Atoms* 377 (2016) 94–98.
- [30] A. Misra, J.P. Hirth, R.G. Hoagland, Length-scale-dependent deformation mechanisms in incoherent metallic multilayered composites, *Acta Mater.* 53 (2005) 4817–4824.